Polymer Chemistry

Accepted Manuscript

ROYAL SOCIETY OF CHEMISTRY

www.rsc.org/polymers

Polymer Chemistry

Dynamic Article Links ►

Cite this: DOI: 10.1039/c0xx00000x

www.rsc.org/xxxxxx

PAPER

Highly thermal stable hydrogels derived from monolayered two-dimensional supramolecular polymers

Tian-You Zhou,[a] Qiao-Yan Qi,[a] Qiao-Ling Zhao,[a] Jie Fu,[a] Yi Liu,[b] Zhi Ma[a] and Xin Zhao*[a]

Received (in XXX, XXX) Xth XXXXXXXXX 20XX, Accepted Xth XXXXXXXXX 20XX

DOI: 10.1039/b000000x

It has been anticipated that the properties of materials would be dramatically influenced if their structures could be confined to two-dimensional (2D) space. A representative example is graphene. However, for synthetic 2D materials, such influences have rarely been demonstrated. In this work, a rare example of how the 2D monolayer structure can impact the properties of bulk materials has been demonstrated by the construction of 2D supramolecular polymers (SPs) and their utilizations for the fabrication of hydrogels. Holding the intrinsic 2D structures, the as-prepared hydrogels exhibited exceptional thermal stability (> 180 °C), as revealed by inversion test and variable-temperature rheological study. The microstructures and morphologies of the 2D SPs have been extensively characterized by NMR, dynamic light scattering, small-angel X-ray scattering, transmission electron microscopy, and atomic force microscopy. Furthermore, molecular dynamic simulations were also performed to shed light on the formation mechanism of the hydrogels.

Introduction

The recent boom of research interests on graphene[1] has spurred great research interests on two dimensional (2D) synthetic materials in recognition of the specific atom arrangement, large surface area and extremely high aspect ratio of 2D structures.[2] Due to the substantial synthetic challenges, much of the efforts have been devoted towards controlled synthesis of isolated, layered 2D structures, broadly known as 2D polymers. Several 2D polymers have been constructed via chemical synthesis[3] or self-assembly[4] over the past two years, some of which possess impressive atomic structural precision within individual layers. Despite these great synthetic advances, emergent material properties derived from the unique 2D structures of such polymers still remain to be demonstrated.

Hydrogels, a family of jelly-like soft materials fabricated from gelation of water by specific molecules, have been extensively studied in the past decades because of their widespread applications in biomaterials,[5] chemosensors,[6] and separation technology.[7] A general mechanism for the formation of hydrogels is the immobilization of water molecules in three-dimensional (3D) networks which are created by entanglement of linear polymers or nanofibers self-assembled from small molecules. The thermal stabilities of hydrogels are usually quite low, especially for the hydrogels fabricated from self-assembly of small molecules, which prevent them from being used at elevated temperatures.[8]

In this article, we demonstrate a rare example of how the 2D monolayer structure can impact the properties of bulk materials by the construction of 2D supramolecular polymers (SPs) and their utilizations for the formation of hydrogels with exceptional thermal stability (Scheme 1). These hydrogels with intrinsic 2D periodical structure exhibit extremely high thermal stabilities. The gel phase and elasticity are maintained even at 180 °C, significantly above the boiling point of water, demonstrating that the thermal stability of hydrogel could be significantly enhanced by taking advantage of the unique features of 2D structure. The building blocks for the construction of 2D SPs were designed by incorporating three phenyl-pyridinium (PP) units into the para-positions of triphenylamine skeleton (**1** and **2**, Scheme 1). The dimerization of phenyl-pyridinium (PP) units can be considerably enhanced by the encapsulation of two PP units in the cavity of a CB[8] molecule,[9] an approach employing the potent cucurbit[8]uril (CB[8])-based host-guest chemistry.[10] As revealed by our previous work,[9] the two PP units should adopt a head-to-tail arrangement in the cavity of CB[8]. This advantage removes the requirement to introduce steric groups into the skeleton of the monomer, which is a must in the first example of 2D SP reported by us recently.[4a] In that system dimerization of the whole monomer was observed, as a result of the head-to-head arrangement of the 4,4'-bipyridin-1-ium (BP) units in the cavity of CB[8] when steric groups were not introduced. DFT calculations revealed that these triphenylamine-based building blocks adopted a C_3 symmetric conformation with coplanar arrangement of the three N-Aryl bonds (Fig. S1, ESI), which could facilitate the formation of extended 2D networks with hexagonal pores.

Results and discussion

Characterization of the assembled structures in solution phase

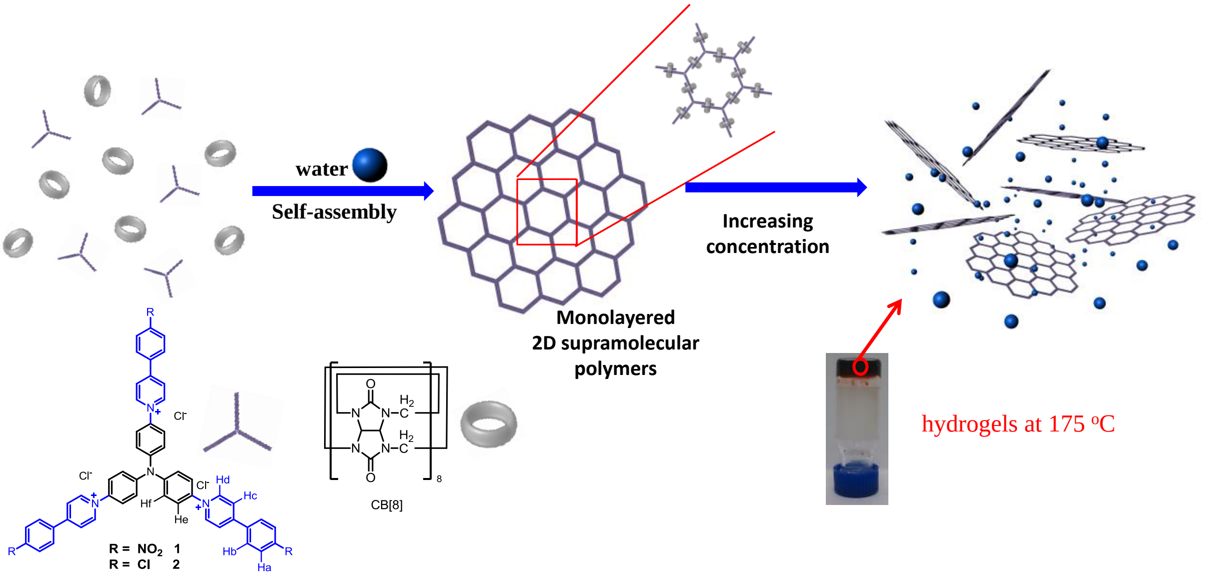

Scheme 1 Structures of building blocks **1**, **2** and CB[8], and cartoon representations of the formation of 2D SPs and hydrogels.

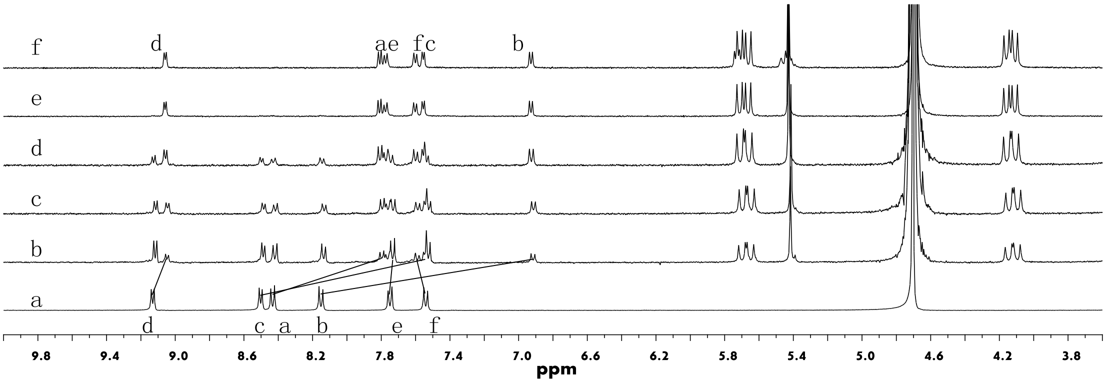

Fig. 1 ^{1}H NMR spectra (500 MHz) of (a) **1** (0.5 mM), (b) **1** + CB[8] (0.3 equiv), (c) **1** + CB[8] (0.75 equiv), (d) **1** + CB[8] (1.1 equiv), (e) **1** + CB[8] (1.5 equiv), and (f) **1** + CB[8] (1.8 equiv) in D_2O at 25 °C.

The binding between building block **1** and CB[8] was first investigated by ^{1}H NMR titration experiment (Fig. 1). Following the addition of CB[8] into a solution of **1** in D_2O, the intensities of protons (H_a-H_d) of PP units decreased while the signals corresponding to the protons (H_e and H_f) of triphenyl amine segment almost kept unchanged. At the same time, a new set of signals grew up in the range of 9.1-6.8 ppm. This new set of signals was attributed to the encapsulated PP units in the cavity of CB[8], for which the rate of interchange between encapsulated and uncapsulated **1** was slower than the NMR time scale.[11] The binding stoichiometry between **1** and CB[8] was revealed to be 2:3 by Job's plot (Fig. S2, ESI), which was also reflected by the ^{1}H NMR titration experiment: no further change in the signals was observed after the ratio of **1** to CB[8] reached 2:3. The dimerization of PP units in the cavity of CB[8] was further corroborated by 2D ^{1}H NMR nuclear overhauser effect spectroscopy (NOESY). Through-space correlations were observed between H_a and H_d, and H_b and H_d (Fig. S3, ESI), clearly indicating a head-to-tail arrangement of two PP units in the cavity of one CB[8] molecule. Driven by such host-guest interaction, the formation of extended honeycomb-like 2D networks could be expected, as a result of the precise direction control offered by the rigid skeleton of the building blocks. Compound **2** exhibited similar complexation behavior as those of **1** when mixed with CB[8] (Fig. S4-S6, ESI).

The formation of polymeric structures in solution was evidenced by dynamic light scattering (DLS). With the increase of concentration, the hydrodynamic diameter (D_h) of the mixture of **1** and CB[8] (2:3) in water increased sharply within the low concentration range (lower than 0.05 mM) and then became much more smooth and finally reached a plateau value around 1100 nm at higher concentrations (Fig. S7, ESI). The mixture of **2** and CB[8] also gave similar trend (Fig. S8, ESI). These results suggested that supramolecular polymers formed even at very low concentration and reached equilibrium at high concentration. It is a typical feature of self-assembled systems which are under thermodynamic control.

The molecular weights of the supramolecular polymers were estimated by static light scattering (SLS) experiment. It was also found that their molecular weights increased monotonically with the concentrations of the stoichiometric (2:3) mixtures of [**1** + CB[8]] and [**2** + CB[8]] (Fig. S9, ESI). At the highest concentration recorded (0.45 mM for **1** and **2**), the molecular weights were estimated to be 1.36 × 10^6 and 8.5 × 10^5 g/mol, corresponding to degrees of polymerization of 462 and 292 for the 2D polymers fabricated from **1** and **2**, respectively.

The formation of highly thermal stable hydrogels

When the concentrations of the self-assembled systems were further increased, formation of hydrogels was observed (Fig.S10-11, ESI). The critical gelation concentrations of the hydrogels were estimated to be ca. 2.0 mM (6.5 wt.%) for **1**-CB[8] and 2.5 mM (7.8 wt.%) for **2**-CB[8], respectively. Notably, these hydrogels exhibited extremely high thermal stabilities. The gel state could still be maintained even at 175 °C for the hydrogel fabricated from **1** and CB[8] under ambient atmosphere in a sealed tube. Furthermore, no hydrogel collapse was observed after the as-prepared hydrogel was sonicated for 10 minutes. The hydrogel fabricated from **2** and CB[8] also exhibited comparable high thermal stability. The high thermal stabilities of the supramolecular structures in solution were also confirmed by variable-temperature ^{1}H NMR studies. When the temperature was increased from 25 to 75 °C, no observable changes were detected for the chemical shifts and shape of the signals of the SP spectra, suggesting the 2D polymeric structures were maintained at this temperature (Fig. S12-13, ESI). Although ^{1}H NMR experiments at higher temperature were not conducted on account of pressure buildup in the NMR tube, the SPs were expected to remain stable in solution at temperatures well above 75 °C. In addition, the apparent binding constants (K_a) were determined by the fitting the data obtained from UV-vis titration experiments at 25 and 75 °C, respectively. Both of the SPs exhibited high binding strength. At 25 °C **1**-CB[8] held a K_a value of 1.68 ($\pm$0.18) $\times 10^{12}$ M^{-2} and for **2**-CB[8] it was 6.75 ($\pm$ 0.55) $\times 10^{12}$ M^{-2}. As temperature increased to 75 °C, K_a for **1**-CB[8] almost remained (1.37 ($\pm$ 0.05)$\times 10^{12}$ M^{-2}), while that for **2**-CB[8] slightly decreased to 6.08 ($\pm$0.85) $\times 10^{11}$ M^{-2}, indicating again the high thermal stability of the SPs (Fig. S14, ESI).

In order to get some insights to the properties of the hydrogels, rheological properties of the hydrogels were first investigated at 25 and 80 °C under ambient atmosphere, respectively.[12] At the two temperatures, both hydrogels exhibited higher storage modulus (G′) than loss modulus (G″) over the whole range of scanning frequency recorded (Fig. S15, ESI). This result clearly indicated that these hydrogels exhibited typical elastic property and the elasticity was maintained at elevated temperature. Temperature-dependent rheological experiments were further performed to get deeper insight into the thermal stabilities of the hydrogels. This experiment was carried out in a sealed nitrogen atmosphere under 50 bar pressure to avoid the evaporation of water. The following observations confirmed the high thermal stabilities of both hydrogels: (i) the storage modulus of the hydrogels was always higher than their loss modulus in the whole range of temperature recorded (30-180 °C); (ii) the values of both storage modulus and loss modulus of the hydrogels remained nearly constant within the whole temperature range (Fig. 2).

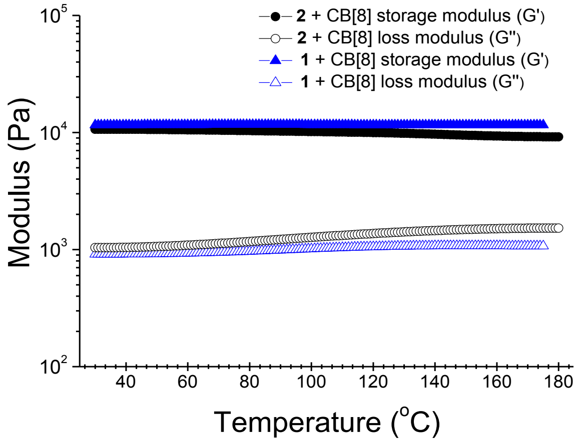

Fig. 2 Temperature-dependent storage modulus (G′) and loss modulus (G″) for hydrogels fabricated from CB[8] and **1** or **2** (50 bar, 1 Hz; 2 ℃ min^{-1}). The concentrations are 16.4 wt.% for **1**-CB[8] and 15.6 wt.% for **2**-CB[8], respectively. The molar ratio for CB[8] to **1** or **2** was 2:3.

The morphology of the xerogels after water being evaporated was examined by scanning electron microscopy (SEM). Layered flakes were observed, consistent with the postulation that the hydrogels were derived from 2D sheets (Fig. S16, ESI). Polarized optical microscopy (POM) study on the xerogels revealed birefringence textures corresponding to crystalline features (Fig. S17, ESI), suggestive of well-ordered internal microstructures of these hydrogels. Hydrogel was regenerated when water was introduced into the xerogel fabricated from **1** and CB[8], indicating re-hydration of the dehydrated 2D SP structures.

The evidence for the formation of single-layer 2D sheets

The extremely high thermal stabilities of these hydrogels were attributed to their distinctive formation mechanism, which was proposed to be driven by the interactions between water molecules and the extraordinarily large surface of the 2D polymeric structures. It was markedly different from the conventional hydrogels reported previously, which were usually generated through 3D entangling of linear fiber-like structures. In order to reveal the formation of 2D supramolecular polymer layers, a variety of techniques have been used to characterize the structures of the materials formed through the self-assembly of CB[8] and **1** or **2** in water. The morphology of the self-assembled structures was first characterized by transmission electron microscopy (TEM). As can be seen in Figure 3a, sheet-like structures can be observed for the sample prepared from [**1** + CB[8] (2:3)]. The contrast between the sheets and the TEM substrate (copper grid-supported carbon film) was very low, consistent with the ultra small thickness of the single layer sheets. Larger area sheets with lateral sizes up to several micrometers were also observed at higher concentration (Fig. 3b). Similar TEM results were also obtained for the sample prepared from [**2** + CB[8] (2:3)] (Fig. S18, ESI). Most notably, the honeycomb units with a pore size of around 3.6 nm could be observed by high resolution (HR)-TEM (Figure 3c), which gave direct evidence for the formation of the proposed 2D network. Since the thicknesses of the sheets could not be estimated from TEM, atomic force microscopy (AFM) was employed to characterize the sheet-like assemblies. Flat and uniform sheets were observed by AFM measurements, with thicknesses of 2.02 and 2.21 nm for the SPs fabricated from **1** and **2** with CB[8], respectively (Figure 3d and Fig. S19, ESI). The values were very close to the theoretical thicknesses of the expected monolayered 2D sheets determined by the outer diameter of CB[8] (Fig. 3e).[13]

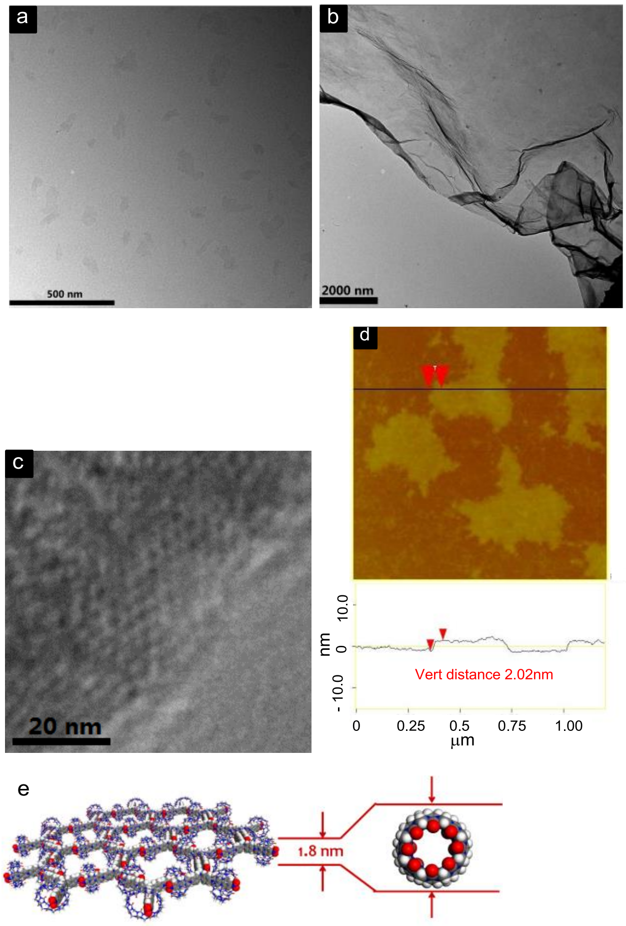

Fig. 3 TEM images of samples of (a) **1** (0.05 mM) and CB[8] (0.075 mM) and (b) **1** (0.25 mM) and CB[8] (0.375 mM), (c) HR-TEM image of the sheet, indicating its honeycomb-like microstructure, and (d) tapping-mode AFM image and cross-section analysis of the sample of [**1** + CB[8] (2:3)], and (e) theoretical thickness of the monolayered 2D SPs. The concentration was 0.05 mM for **1**.

The evidence for long-range ordered 2D periodicity in the 2D SPs

A key criterion for a true 2D polymer is the existence of long-range ordered periodicity in two dimensions. In order to prove that the sheets generated by the self-assembly of CB[8] and **1** or **2** did hold periodic 2D polymeric structures, small angle X-ray scattering (SAXS) experiments were carried out. For the sample fabricated from **1** and CB[8],[14] a scattering peak corresponding to *d* spacing of 3.61 nm (100) was observed (Figure 4a). Moreover, a (200) scattering peak was also observed at *d* spacing of 1.81 nm, further confirming the existence of a periodic size of 3.61 nm. In the case of the sample prepared from **2** and CB[8], scattering peaks corresponding to (100) and (200) were observed at 3.49 and 1.73 nm, respectively (Fig. 4c). Semiempirical calculations at PM3 level revealed that theoretical pore diameter of the expected honeycomb structure was 3.60 nm for both of the SPs fabricated from the co-assembly of CB[8] with **1** or **2**. The experimentally obtained values agreed well with the theoretical ones, corroborating the formation of the expected 2D networks with well-ordered internal microstructure. These scattering peaks could still be observed when the samples were heated to 85 °C (Figure 4b and 4d), suggesting that the 2D networks remained intact at elevated temperature. It indicated again the high thermal stabilities of these 2D supramolecular polymers.

In order to shed light on the formation mechanism of the hydrogels, molecular dynamic simulations were performed for the hydrogel formed from **1** and CB[8] (Fig. 5, see more details in ESI). A snapshot of a (4x4) segment of the 2D layer revealed that water molecules mainly distributed near the skeleton of the honeycomb structure. In contrast, the pore centers have lowest distribution density of water molecules. This result suggests that

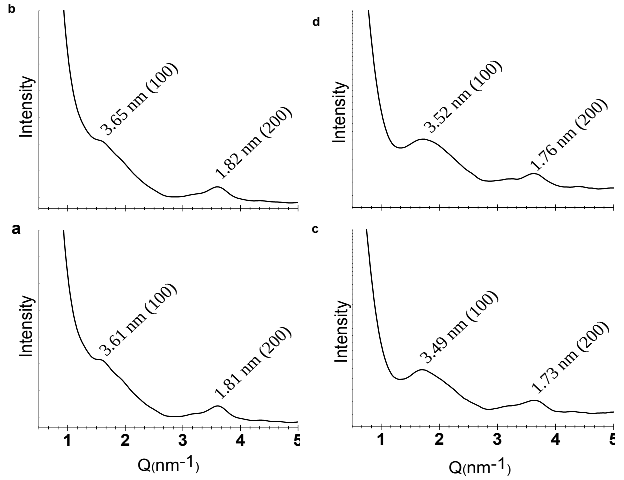

Fig. 4 SAXS patterns of the sample prepared from a hydrogel of **1** and CB[8] (13.0 wt.%) in water (pH = 7) at (a) 25 °C, and (b) 85 °C; And SAXS patterns of the sample prepared from a hydrogel of **2** and CB[8] (9.36 wt.%) in water (pH = 7) at (c) 25 °C and (d) 85 °C.

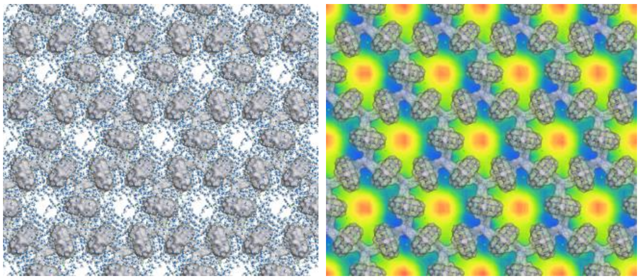

Fig. 5 Left: A snapshot of the simulated hydrogel formed from **1** and CB[8]. The skeleton is illustrated by Connolly Surface for clarity. The oxygen atoms of H_2O are represented by the blue-colored particles, the hydrogen atoms are represented by the gray-colored particles and Cl^- ions are represented by the green-colored particles. Right: The statistic slice of the density field of H_2O to display water distribution on the 2D structure. Blue color shows the relatively high density of H_2O and red color shows the relatively low density of H_2O, indicating that water molecules are more distributed near the skeleton of 2D SP.

the 2D supramolecular polymers have high affinity to water molecules, which should be ascribed to the formation of hydrogen bonds with the O and N atoms of CB[8] and NO_2 groups of PP units (for building block **1**). Through these hydrogen-bonding interactions, a huge number of water molecules could be localized on surfaces of the monolayered sheets, which further extended to produce hydrogels. In this context, the high thermal stability of the hydrogel could be attributed to the extraordinarily large surface areas of the 2D structures, which provide the maximum interaction sites for the formation of hydrogen bonds. Compared to **2**-CB[8], **1**-CB[8]exhibited lower critical gelation concentration and higher molecular weights and storage modulus. It could be attributed to the additional hydrogen-bonding sites provided by nitro group of compound **1**.

Conclusions

In conclusion, the significant impact of a unique 2D structure on the performance of soft materials has been demonstrated. Different from traditional hydrogels which were usually formed by 3D entanglement of flexible linear structures, the hydrogels reported here were generated from monolayered 2D supramolecular polymers without any flexible side chains. Thanks to the extraordinarily large surface areas of the 2D structures, maximum interaction sites could be provided to immobilize water molecules on their surface and thus the thermal stabilities of hydrogels were enhanced significantly. Currently the research on synthetic 2D polymers is still at a very early stage. Much attention has been paid to the construction and characterizations of 2D structures while their properties and applications are awaiting further exploration. The highly thermostable hydrogels demonstrated in this work reveal that the unique features of 2D structures could be essential for the fabrication of unconventional functional materials. As this work takes advantage of only one feature of 2D structures, i.e. large surface area, we believe that the other features of this type of structure will also endow 2D polymer-based materials with unique properties and functions. For example, the long-range ordered periodicity in 2D space could be exploited for the construction of well-ordered arrays of sensors to achieve ultrahigh sensitivity. This potential is under investigation in our laboratory.

Acknowledgements

We thank the National Natural Science Foundation of China (Nos. 21172249 and 91127007) for financial support. Y.L. acknowledges the support from the Molecular Foundry, Lawrence Berkeley National Laboratory, supported by the Office of Science, Office of Basic Energy Sciences, Scientific User Facilities Division, of the U.S. Department of Energy under Contract No. DE-AC02-05CH11231. We also thank Prof. Zhan-Ting Li and Mr. Jia Tian (Fudan University) for their help in preparing the manuscript and Prof. Li-Zhu Wu (Technical Institute of Physics and Chemistry) for her helpful advice.

Notes and references

[a] *Key Laboratory of Synthetic and Self-Assembly Chemistry for Organic Functional Molecules, Shanghai Institute of Organic Chemistry, Chinese Academy of Sciences, 345 Lingling Road, Shanghai, 200032, China.*
E-mail: xzhao@mail.sioc.ac.cn
[b] *The Molecular Foundry, Lawrence Berkeley National Laboratory,*
One Cyclotron Road, MS 67R6110, Berkeley, CA 94720, USA.

† Electronic Supplementary Information (ESI) available: Synthesis and characterizations of compounds, ^1H NMR 2D NOESY spectra, variable-temperature ^1H NMR spectra, SEM image, POM image, pictures for the hydrogels, and additional rheological experiment, ^1H NMR titration spectra and TEM images. See DOI: 10.1039/b000000x/

1 (a) K. S. Novoselov, A. K. Geim, S. V. Morozov, D. Jiang, Y. Zhang, S. V. Dubonos, I. V. Grigorieva and A. A. Firsov, *Science*, 2004, **306**, 666; (b) K. S. Novoselov, A. K. Geim, S. V. Morozov, D. Jiang, M. I. Katsnelson, I. V. Grigorieva, S. V. Dubonos and A. A. Firsov, *Nature*, 2005, **438**, 197; (c) M. J. Allen, V. C. Tung and R. B. Kaner, *Chem. Rev.*, 2010, **110**, 132.

2 (a) J. Sakamoto, J. van Heijst, O. Lukin and A. D. Schlüter, *Angew. Chem. Int. Ed.*, 2009, **48**, 1030; (b) R. Mas-Ballesté, C. Gómez-Navarro, J. Gómez-Herrero and F. Zamora, *Nanoscale*, 2011, **3**, 20.

3 (a) T.-Y. Zhou, F. Lin, Z.-T. Li and X. Zhao, *Macromolecules*, 2013, **46**, 7745; (b) P. Kissel, R. Erni, W. B. Schweizer, M. D. Rossell, B. T. King, T. Bauer, S. Gotzinger, A. D. Schlüter and J. Sakamoto, *Nat. Chem.*, 2012, **4**, 287; (c) P. Kissel, D. J. Murray, W. J. Wulftange, V. J. Catalano and B. T. King, *Nat. Chem.*, 2014, **6**, 774; (d) M. J. Kory, M. Wörle, T. Weber, P. Payamyar, S. W. van de Poll, J. Dshemuchadse, N. Trapp and A. D. Schlüter, *Nat. Chem.*, 2014, **6**, 779; (e) K. Baek, G. Yun, Y. Kim, D. Kim, R. Hota, I. Hwang, D. Xu, Y. H. Ko, G. H. Gu, J. H. Suh, C. G. Park, B. J. Sung and K. Kim, *J. Am. Chem. Soc.*, 2013, **135,** 6523.

4 (a) K.-D. Zhang, J. Tian, D. Hanifi, Y. Zhang, A. C.-H. Sue, T.-Y. Zhou, L. Zhang, X. Zhao, Y. Liu and Z.-T Li, *J. Am. Chem. Soc.*, 2013, **135**, 17913; (b) L. Zhang. T.-Y. Zhou, J. Tian, H. Wang, D.-W. Zhang, X. Zhao and Z.-T. Li, *Polym. Chem.*, 2014, **5**, 4715; (c) X. Zhang, C.-B. Nie, T.-Y. Zhou, Q.-Y. Qi, J. Fu, X.-Z. Wang, L. Dai, Y. Chen and X. Zhao, *Polym. Chem.*, 2015, **6**, DOI: 10.1039/C4PY01669F.

5 (a) O. P. Oommen, S. Wang, M. Kisiel, M. Sloff, J. Hilborn and O. P. Varghese, *Adv. Funct. Mater.*, 2013, **23**, 1273; (b) N. Annabi, K. Tsang, S. M. Mithieux, M. Nikkhah, A. Ameri, A. Khademhosseini and A. S. Weiss, *Adv. Funct. Mater.*, 2013, **23,** 4950; (c) Y. Liu and M. B. Chan-Park, *Biomaterials*, 2009, **30**, 196.

6 (a) D. Zhai, B. Liu, Y. Shi, L. Pan, Y. Wang, W. Li, R. Zhang and G. Yu, *Acs Nano*, 2013, **7**, 3540; (b) D. Pussak, D. Ponader, S. Mosca, S. V. Ruiz, L. Hartmann and S. Schmidt, *Angew. Chem. Int. Ed.*, 2013, **52**, 6084; (c) S. Bhowmik, B. N. Ghosh, V. Marjomaki and K. Rissanen, *J. Am. Chem. Soc.*, 2014, **136**, 5543.

7 (a) Y. Liu, S. Yu, H. Wu, Y. Li, S. Wang, Z. Tian and Z. Jiang, *J. Membrane Sci.*, 2014, **469**, 198; (b) F. Lu, Y. Chen, N. Liu, Y. Cao, L. Xu, Y. Wei and L. Feng, *Rsc Adv.*, 2014, **4**, 32544.

8 (a) M. Guo, L. Pitet, H. Wyss, M. Vos, P. Y. W. Dankers and E. W. Meijer, *J. Am. Chem. Soc.*, 2014**, 136**, 6969; (b) Z. Lv, L. Chang, X. Long, J. Liu, Y. Xiang, J. Liu, J. Liu, H. Deng, L. Deng and A. Dong, *Carbohydr. Polym.*, 2014, **108**, 26; (c) F. Lv, L. Mao and T. Liu, *Mater. Sci. Eng. C*, 2014, **43**, 221; (d) G. Azevedo, B. Domingues, H. Abreu, I. Sousa-Pinto, G. Feio and L. Hilliou, *Carbohydr. Polym.*, 2014, **108**, 140.

9 Y. Zhang, T.-Y. Zhou, K.-D. Zhang, J.-L. Dai, Y.-Y. Zhu and X. Zhao, *Chem. Asian. J.*, 2014, **9**, 1530.

10 (a) C. Yang, T. Mori, Y. Origane, Y. H. Ko, N. Selvapalam, K. Kim and Y. Inoue, *J. Am. Chem. Soc.*, 2008, **130**, 8574; (b) Y. H. Ko, Y. Kim, H. Kim and K. Kim, *Chem. Asian. J.*, 2011, **6**, 652; (c) Z.-J. Ding, H.-Y. Zhang, L.-H. Wang, F. Ding and Y. Liu, *Org. Lett.*, 2011, **13**, 856; (d) Q. Wang, Y. Chen and Y. Liu, *Polym. Chem.*, 2013, **4**, 4192; (e) W. S. Jeon, H. J. Kim, C. Lee and K. Kim, *Chem. Commun.*, 2002, 1828; (f) A. Y. Ziganshina, Y. H. Ko, W. S. Jeon and K. Kim, *Chem. Commun.*, 2004, 806; (g) Y. Lan, Y. Wu, A. Karas and O. A. Scherman, *Angew. Chem. Int. Ed.*, 2014, **53**, 2166; (h) Z. Huang, L. Yang, Y. Liu, Z. Wang, O. A. Scherman and X. Zhang, *Angew. Chem. Int. Ed.*, 2014, **53**, 5351; (i) J. R. McKee, E. A. Appel, J. Seitsonen,

E. Kontturi, O. A. Scherman and O. Ikkala, *Adv. Funct. Mater.*, 2014, **24**, 2706; (j) F. Biedermann, I. Ross and O. A. Scherman, *Polym. Chem.*, 2014, **5**, 5375; (k) J. del Barrio, P. N. Horton, D. Lairez, G. O. Lloyd, C. Toprakcioglu and O. A. Scherman, *J. Am. Chem. Soc.*, 2013, **135**, 11760; (l) F. Biedermann, M. Vendruscolo, O. A. Scherman, A. De Simone and W. M. Nau, *J. Am. Chem. Soc.*, 2013, **135**, 14879; (m) H. Qian, D.-S. Guo and Y. Liu, *Chem. Eur. J.*, 2012, **18**, 5087; (n) C. Yang, C. Ke, W. T. Liang, G. Fukuhara, T. Mori, Y. Liu and Y. Inoue, *J. Am. Chem. Soc.*, 2011, **133**, 13786; (o) H. Yang, B. Yuan, X. Zhang and O. A. Scherman, *Acc. Chem. Res.*, 2014, **47**, 2106; (p) H. Yang, Z. Ma, Z. Wang and X. Zhang, *Polym. Chem.*, 2014, **5**, 1471; (q) F. Lin, T.-G. Zhan, T.-Y. Zhou, K.-D. Zhang, G.-Y. Li, J. Wu and X. Zhao, *Chem. Commun.*, 2014, **50**, 7982.

11 Z.-J. Zhang, H.-Y. Zhang, L. Chen and Y. Liu, *J. Org. Chem.*, 2011, **76**, 8270.

12 (a) G. Yu, X. Yan, C. Han and F. Huang, *Chem. Soc. Rev.*, 2013, **42**, 6697; (b) X. Yan, D. Xu, X. Chi, J. Chen, S. Dong, X. Ding, Y. Yu and F. Huang, *Adv. Mater.*, 2012, **24**, 362; (c) J. W. Steed, *Chem. Soc. Rev.*, 2010, **39**, 3686.

13 K. Kim, N. Selvapalam, Y. H. Ko, K. M. Park, D. Kim and J. Kim, *Chem. Soc. Rev.*, 2007, **36**, 267.

14 In order to inject the samples into the sample tube of SAXS, partially gelated samples were prepared for SAXS experiment by dispersing the as-prepared hydrogels in water.